Nitrous Oxide

International Edition: DOI: 10.1002/anie.201908333
German Edition: DOI: 10.1002/ange.201908333

# Rhodium(I) Pincer Complexes of Nitrous Oxide

*Matthew R. Gyton, Baptiste Leforestier, and Adrian B. Chaplin**

***Abstract:*** *The synthesis of two well-defined rhodium(I) complexes of nitrous oxide ($N_2O$) is reported. These normally elusive adducts are stable in the solid state and persist in solution at ambient temperature, enabling comprehensive structural interrogation by $^{15}N$ NMR and IR spectroscopy, and single-crystal X-ray diffraction. These methods evidence coordination of $N_2O$ through the terminal nitrogen atom in a linear fashion and are supplemented by a computational energy decomposition analysis, which provides further insights into the nature of the Rh–$N_2O$ interaction.*

The synthetic exploitation of nitrous oxide ($N_2O$) is an enduring challenge that draws topical interest as a means to remediate the detrimental impact emission of this kinetically stable gas on the environment.[1] Whilst the application of homogenous transition-metal complexes is an attractive prospect, the underpinning inorganic chemistry is conspicuously under-developed.[2] Indeed, the number of discrete transition-metal complexes of $N_2O$ is currently limited to a handful of examples (**A**–**D**), of which only two have been structurally characterised in the solid state using X-ray diffraction (Figure 1).[3–7] This paucity is attributed to the extremely poor ligand properties of $N_2O$, conferred by a low dipole moment, weak σ-donor and π-acceptor characteristics, and the propensity of these adducts for subsequent N–N or N–O bond cleavage.[2]

Inspired by work by Brookhart and Caulton,[8,9] and building upon that conducted in our laboratories,[10] we chose cationic phosphine-based pincer complexes of rhodium(I) as a platform for studying the coordination chemistry of $N_2O$. Our approach utilises dimeric $[\{Rh(pincer)\}_2(\mu\text{-}\eta^2\text{:}\eta^2\text{-COD})][BAr^F{}_4]_2$ (**1a**, pincer = 2,6-$(tBu_2PO)_2C_5H_3N$; **1b**, pincer = 2,6-$(tBu_2PCH_2)_2C_5H_3N$; COD = cyclooctadiene, $Ar^F$ = 3,5-$(CF_3)_2C_6H_3$) as synthons for reactive $\{Rh(pincer)\}^+$ fragments in the weakly coordinating solvent 1,2-$F_2C_6H_4$ (DFB).[11] Satisfactorily, reactions of **1** with $N_2O$ (1.5 bar) at room temperature afforded well-defined adducts $[Rh(pincer)(N_2O)][BAr^F{}_4]$ **2** in quantitative yield by $^{31}P$ NMR spectroscopy, as evidenced by resonances at $\delta$ 210.4 (**2a**, $^1J_{RhP}$ = 134 Hz, $t$ < 3 h)/ $\delta$ 70.9 (**2b**, $^1J_{RhP}$ = 127 Hz, $t$ < 5 min) that display diagnostic $^{103}Rh$ coupling (Figure 1). These Rh–$N_2O$ complexes were subsequently isolated as analytically pure materials in good yield on precipitation with hexane at low temperature and extensively characterised (**2a**, 65%; **2b** 78%). Both can be stored under argon in the solid state, but decompose slowly in DFB solution at room temperature (**2a**, $t_{50\%dec} \approx 4.0$ h; **2b**, $t_{50\%dec} \approx 2.5$ h), with generation of the known dinitrogen complexes $[Rh(pincer)(N_2)][BAr^F{}_4]$ (**3a**, $\delta$ 211.3, $^1J_{RhP}$ = 133 Hz; **3b**, $\delta$ 71.2, $^1J_{RhP}$ = 126 Hz).[10,12] By drawing parallels with the reaction of a neutral rhodium PNP analogue with $N_2O$, where formation of a discrete adduct is inferred but not experimentally corroborated, we suggest **2** decomposes by a bimetallic oxygen atom transfer mechanism that is initiated by dissociation of $N_2O$ and proceeds via $\{(pincer)Rh^{II}\text{–}N{=}N\text{–}O\text{–}Rh^{II}(pincer)\}^{2+}$.[9,13] Consistent with this assertion, enhanced solution stability was observed under a $N_2O$ atmosphere (2%/30% decomposition of **2a**/**b** after 24 h).

The structures of **2** were definitively established in DFB solution using $^{15}N$ NMR spectroscopy, aided by samples prepared using isotopically labelled $^{15}N_2O$ (98% $^{15}N$, Figure 2 and the Supporting Information). Intact coordination of $N_2O$ through the terminal nitrogen atom is evident by an upfield shift of $\Delta\delta$ 43.3/37.0 for the corresponding $^{15}N$ resonances, comparable to that of **B**,[4] which exhibit $^1J_{RhN}$ coupling of

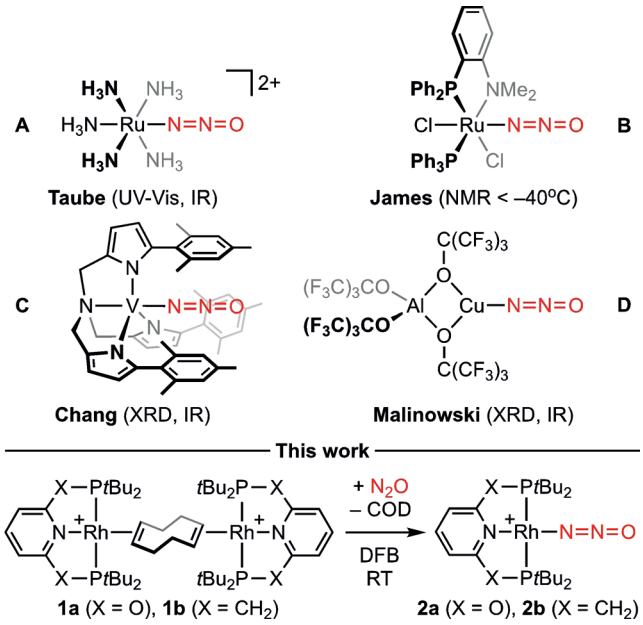


***Figure 1.*** Well-defined transition-metal complexes of nitrous oxide. Weakly coordinating $[BAr^F{}_4]^-$ anions have been omitted from the reaction scheme for clarity.

[*] Dr. M. R. Gyton, B. Leforestier, Dr. A. B. Chaplin
Department of Chemistry, University of Warwick
Gibbet Hill Road, Coventry CV4 7AL (UK)
E-mail: a.b.chaplin@warwick.ac.uk
Homepage: http://go.warwick.ac.uk/abchaplin
Supporting information and the ORCID identification number(s) for the author(s) of this article can be found under: https://doi.org/10.1002/anie.201908333.

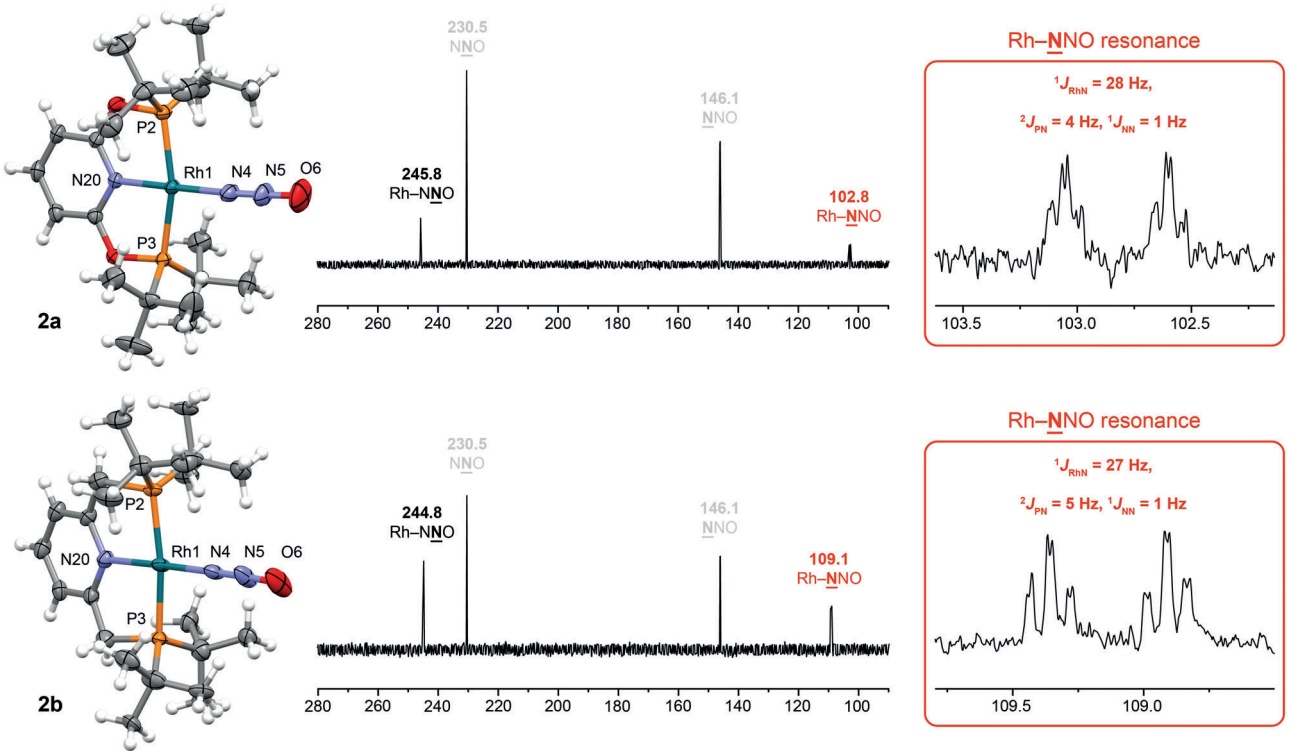


***Figure 2.*** Solid-state structures (150 K) and $^{15}$N NMR spectra ($^{15}N_2O$ atmosphere, DFB, 61 MHz, 298 K) of **2**. Thermal ellipsoids drawn at 50% (**2a**) and 30% (**2b**) probability; minor disordered components (pincer ligand in **2b**) and anions omitted for clarity. Selected bond lengths and angles: **2a** Rh1–P2 2.2677(5) Å, Rh1–P3 2.2688(5) Å, Rh1–N4 1.981(2) Å, N4–N5 1.108(3) Å, N5–O6 1.194(3) Å, Rh1–N20 2.007(2); N20–Rh1–N4 178.05(8)°, Rh1–N4–N5 173.4(2)°, N4–N5–O6 178.5(3)°; **2b** Rh1–P2 2.282(2) Å, Rh1–P3 2.288(2) Å, Rh1–N4 1.962(7) Å, N4–N5 1.111(11) Å, N5–O6 1.192(11) Å, Rh1–N20/N20A 2.071(7)/2.052(8) Å; N20/N20A–Rh1–N4 178.1(5)/175.4(5)°, Rh1–N4–N5 176.8(11)°, N4–N5–O6 178.7(14)°.[22]

28/27 Hz[14] and $^{2}J_{PN}$ coupling of 4/5 Hz for **2a/b**, respectively. The internal $^{15}$N resonances are conversely shifted downfield by $\Delta\delta$ 15.3/14.3, but retain coupling to both $^{103}$Rh ($^{2}J_{RhN}$ = 8 Hz) and $^{31}$P ($^{3}J_{PN}$ = 1 Hz), albeit with commensurate reductions in magnitude. The $^{1}J_{NN}$ coupling constant of free $N_2O$ (9 Hz) is small and appreciably reduced on complexation to rhodium; to the extent that it is only just resolved (1 Hz). Analysis of natural abundance and isotopically labelled (powdered) solid samples of **2** using ATR IR spectroscopy enabled unambiguous assignment of the principal $\nu$(N-N) and $\nu$(N-O) bands of **2a** (2279, 1252 cm$^{-1}$, respectively) and **2b** (2267, 1228 cm$^{-1}$, respectively). The former are significantly blue shifted, relative to the free ligand, whilst the latter are red shifted (2224, 1285 cm$^{-1}$, respectively).[15] Spectra of **2** can also be acquired in DFB and give similar values (full details are provided in the Supporting Information). Higher energy $\nu$(N-N) bands are also observed for **C** and **D**,[5,6] with this phenomenon running contrary to normal expectations for (meaningful) metal-to-ligand π-back bonding.

The solid-state structures of **2a** and **2b** have been determined using single-crystal X-ray diffraction (150 K) and verify that they are both discrete $N_2O$ complexes, with the ligand binding through the terminal nitrogen atom in a linear fashion (Rh–N–N > 173° and N–N–O > 178°; Figure 2). The former is well-ordered, but the latter features an extensively disordered pincer ligand symptomatic of dynamic isomerism in the lattice ($C_2 \rightleftharpoons C_s$ conformations).[16] Whilst this disorder was modelled satisfactorily, the metal–ligand metrics in **2b** are inevitably determined with reduced precision in comparison to **2a**. Nevertheless, the pertinent data associated with coordination of $N_2O$ in **2** point to very similar bonding characteristics. When normalising by the sum of the covalent radii,[17] the extent of the M–N interactions in **2a** (1.981(2) Å) and **2b** (1.962(7) Å) are in close agreement with those previously determined in **C** (2.1389(10) Å) and **D** (1.890(8) Å): $r$(M-N)/[$r$(M) + $r$(N)] = 0.93, **2a**; 0.92, **2b**; 0.95, **C**; 0.93, **D**.[5,6] There is a trend for the N–N bonds (1.108(3)/1.111(11) compared to 1.128 Å) to be shortened and the N–O bonds (1.194(3)/1.192(11) compared to 1.184 Å) to be elongated in **2a/b** relative to free $N_2O$,[15] but these changes are marginal.

Supplementing the experimental work, the geometries and thermodynamics of **2** were interrogated in silico at the DLPNO-CCSD(T)/def2-TZVPP//ωB97X-D3/def2-TZVP(-f) level of theory.[18] Whilst the trend for a longer Rh–N contact in **2a** (2.006 Å) relative to **2b** (1.989 Å) established by X-ray diffraction is reproduced, it is for the former that binding of $N_2O$ is predicted to be most exergonic ($\Delta G_{298K}$ = −68.5 kJ mol$^{-1}$, **2a**; −67.6 kJ mol$^{-1}$ **2b**). The magnitude of these values is consistent with slow exchange on the $^{15}$N NMR timeframe (61 MHz, 298 K; Figure 2), with the difference congruent with the relative rate of decomposition observed in solution. Only very small perturbations to the N–N and N–O bond lengths are computed on coordination (less than 0.005 Å), but the associated vibrations corroborate the experimental pattern and are discernibly blue and red shifted,

  

***Table 1:*** LED results for **2** → {Rh(pincer)}$^+$ + $N_2O$ (kJ mol$^{-1}$).[18]

| | **2a** | **2b** |
|---|---|---|
| $\Delta E_{interaction}$ | −124.8 | −119.8 |
| $E_{dispersion}$ | −70.0 | −76.5 |
| $\Delta E_{Pauli}$ | +476.8 | +519.1 |
| $E_{electrostatic}$ | −359.0 | −385.5 |
| $\Delta E_{orbital}$ | −140.9 | −148.0 |
| $\Delta E_{orbital}$ (σ donation)[a] | −79.8 (57%) | −83.3 (56%) |
| $\Delta E_{orbital}$ (π backbonding)[a] | −56.2 (40%) | −59.2 (40%) |
| $\Delta E_{residual}$ | −31.7 | −33.1 |
| $\Delta E_{preparation}$ | +2.5 | +3.8 |
| $\Delta E_{binding}$ (= $-D_e$) | −122.3 | −120.1 |

[a] Determined by application of the extended transition state method for energy decomposition analysis combined with the natural orbitals for chemical valence theory (ETS-NOCV). The character of the interaction is deduced from visual inspection of the natural orbitals. Percentage of total orbital interaction $\Delta E_{orbital}$ in parenthesis.

respectively (see the Supporting Information). To gain deeper insight into the nature of the Rh–$N_2O$ interaction, a local energy decomposition (LED) analysis was carried out using ORCA 4.1.2. (Table 1; Supporting Information).[18–20] The results reiterate marginally stronger $N_2O$ binding in **2a** ($D_e$ = + 122.3 kJ mol$^{-1}$) compared to **2b** ($D_e$ = + 120.1 kJ mol$^{-1}$) and highlight the important role of dispersion, which accounts for approximately 12% of the total stabilising interactions.[21] The interfragment orbital energies are small and reflect the presence of weak σ-donation and π-back bonding; with the former predominating (ca. 56% vs. 40%). When the two complexes are compared, the combined stabilising interactions are most pronounced for **2b**, but counteracted by even more extensive Pauli repulsion (i.e. sterics) than in **2a**. The latter difference is reconciled by the more obtuse bite angle of the PNP (P–Rh–P = 169.24(8)°, expt) vs. PONOP (P–Rh–P = 162.77(2)°, expt) pincer ligand, which causes greater buttressing between the *t*Bu substituents and the coordinated $N_2O$ ligand.

In summary, the synthesis and comprehensive characterisation of two rhodium(I) pincer complexes of $N_2O$ are reported. Through an unprecedented combination of $^{15}N$ NMR and IR spectroscopy, and single crystal X-ray diffraction the discrete nature of these complexes and the coordination of $N_2O$ to the metal through the terminal nitrogen atom in a linear fashion is unequivocally established. Subtle differences in the characteristics of the Rh–$N_2O$ interaction associated with the ancillary pincer ligand employed have been reconciled using a computational energy-decomposition analysis, which highlights the weakly interacting nature of $N_2O$, the important stabilising role of dispersion interactions, and the effect of steric buttressing with the pincer substituents.

## Acknowledgements

We thank the European Research Council (ERC, grant agreement 637313; M.R.G., B.L., A.B.C.) and Royal Society (UF100592, UF150675, A.B.C.) for financial support. Crystallographic data were collected using an instrument that received funding from the ERC under the European Union's Horizon 2020 research and innovation programme (grant agreement No 637313). Computing facilities were provided by the Scientific Computing Research Technology Platform of the University of Warwick.

## Conflict of interest

The authors declare no conflict of interest.

**Keywords:** coordination chemistry · nitrous oxide · pincer ligands · rhodium · structure elucidation

[1] a) D. S. Reay, E. A. Davidson, K. A. Smith, P. Smith, J. M. Melillo, F. Dentener, P. J. Crutzen, *Nat. Clim. Change* **2012**, *2*, 410–416; b) J. Hansen, M. Sato, *Proc. Natl. Acad. Sci. USA* **2004**, *101*, 16109–16114; c) D. J. Wuebbles, *Science* **2009**, *326*, 56–57; d) A. R. Ravishankara, J. S. Daniel, R. W. Portmann, *Science* **2009**, *326*, 123–125.

[2] a) K. Severin, *Chem. Soc. Rev.* **2015**, *44*, 6375–6386; b) W. B. Tolman, *Angew. Chem. Int. Ed.* **2010**, *49*, 1018–1024; *Angew. Chem.* **2010**, *122*, 1034–1041; c) D.-H. Lee, B. Mondal, K. D. Karlin in *Activation of Small Molecules* (Ed.: W. B. Tolman), Wiley-VCH, Weinheim, **2006**, pp. 43–79.

[3] a) J. N. Armor, H. Taube, *J. Am. Chem. Soc.* **1969**, *91*, 6874–6876; b) F. Paulat, T. Kuschel, C. Näther, V. K. K. Praneeth, O. Sander, N. Lehnert, *Inorg. Chem.* **2004**, *43*, 6979–6994.

[4] C. B. Pamplin, E. S. F. Ma, N. Safari, S. J. Rettig, B. R. James, *J. Am. Chem. Soc.* **2001**, *123*, 8596–8597.

[5] N. A. Piro, M. F. Lichterman, W. H. Harman, C. J. Chang, *J. Am. Chem. Soc.* **2011**, *133*, 2108–2111.

[6] V. Zhuravlev, P. J. Malinowski, *Angew. Chem. Int. Ed.* **2018**, *57*, 11697–11700; *Angew. Chem.* **2018**, *130*, 11871–11874.

[7] For other examples that do not involve formation of a discrete coordination complex see: a) A. Pomowski, W. G. Zumft, P. M. H. Kroneck, O. Einsle, *Nature* **2011**, *477*, 234–237; b) D. J. Xiao, E. D. Bloch, J. A. Mason, W. L. Queen, M. R. Hudson, N. Planas, J. Borycz, A. L. Dzubak, P. Verma, K. Lee, et al., *Nat. Chem.* **2014**, *6*, 590–595.

[8] a) W. H. Bernskoetter, C. K. Schauer, K. I. Goldberg, M. Brookhart, *Science* **2009**, *326*, 553–556; b) M. D. Walter, P. S. White, C. K. Schauer, M. Brookhart, *J. Am. Chem. Soc.* **2013**, *135*, 15933–15947.

[9] a) A. Y. Verat, H. Fan, M. Pink, Y. S. Chen, K. G. Caulton, *Chem. Eur. J.* **2008**, *14*, 7680–7686; b) J. G. Andino, K. G. Caulton, *J. Am. Chem. Soc.* **2011**, *133*, 12576–12583.

[10] M. R. Gyton, T. M. Hood, A. B. Chaplin, *Dalton Trans.* **2019**, *48*, 2877–2880.

[11] S. D. Pike, M. R. Crimmin, A. B. Chaplin, *Chem. Commun.* **2017**, *53*, 3615–3633.

[12] a) G. M. Adams, F. M. Chadwick, S. D. Pike, A. S. Weller, *Dalton Trans.* **2015**, *44*, 6340–6342; b) A. B. Chaplin, A. S. Weller, *Organometallics* **2011**, *30*, 4466–4469.

[13] Correspondingly we suggest paramagnetic rhodium oxyls of the form [Rh$^{II}$(pincer)O]$^+$ are also generated, but we have so far been unable to confirm this experimentally. Time-course data collected under argon is consistent with formation of NMR-silent species and second-order decomposition with respect to **2** (see the Supporting Information). For other precedents for this type of mechanism see: a) J. T. Groves, J. S. Roman, *J. Am. Chem. Soc.* **1995**, *117*, 5594–5595; b) H. Yu, G. Jia, Z. Lin,

  

*Organometallics* **2009**, *28*, 1158 – 1164; c) T. D. Palluccio, E. V. Rybak-Akimova, S. Majumdar, X. Cai, M. Chui, M. Temprado, J. S. Silvia, A. F. Cozzolino, D. Tofan, A. Velian, C. C. Cummins, B. Captain, C. D. Hoff, *J. Am. Chem. Soc.* **2013**, *135*, 11357—11372.

[14] S. Donovan-Mtunzi, R. L. Richards, J. Mason, *J. Chem. Soc. Dalton Trans.* **1984**, 469 – 474.

[15] W. C. Trogler, *Coord. Chem. Rev.* **1999**, *187*, 303 – 327.

[16] T. M. Hood, B. Leforestier, M. R. Gyton, A. B. Chaplin, *Inorg. Chem.* **2019**, *58*, 7593 – 7601.

[17] B. Cordero, V. Gómez, A. E. Platero-Prats, M. Revés, J. Echeverría, E. Cremades, F. Barragán, S. Alvarez, *Dalton Trans.* **2008**, 2832 – 2838.

[18] Only the metal cations are considered. In the case of **2b** there are two possible isomers, related to the conformation the pincer ligand adopts, but for simplicity the discussion is focused exclusively on the lower energy $C_2$-symmetric isomer in the main text. The $C_s$-symmetric isomer is $\Delta G_{298K} = +3.7$ kJ mol$^{-1}$ higher in energy and the LED analysis is provided in the Supporting Information.

[19] a) W. B. Schneider, G. Bistoni, M. Sparta, M. Saitow, C. Riplinger, A. A. Auer, F. Neese, *J. Chem. Theory Comput.* **2016**, *12*, 4778 – 4792; b) A. Altun, F. Neese, G. Bistoni, *J. Chem. Theory Comput.* **2019**, *15*, 215 – 228.

[20] a) F. Neese, *Wiley Interdiscip. Rev.: Comput. Mol. Sci.* **2012**, *2*, 73 – 78; b) F. Neese, *Wiley Interdiscip. Rev.: Comput. Mol. Sci.* **2018**, *8*, e1327.

[21] The important stabilising role of dispersion interactions has also been invoked recently in the formation of structurally related σ-alkane complexes: Q. Lu, F. Neese, G. Bistoni, *Phys. Chem. Chem. Phys.* **2019**, *21*, 11569 – 11577.

[22] CCDC 1938490 and 1938491 contain the supplementary crystallographic data for this paper. These data can be obtained free of charge from The Cambridge Crystallographic Data Centre.

Manuscript received: July 4, 2019
Version of record online: ■■ ■■, ■■■■

  

# Communications

Nitrous Oxide

M. R. Gyton, B. Leforestier, A. B. Chaplin* ——— ■■■■–■■■■

Rhodium(I) Pincer Complexes of Nitrous Oxide

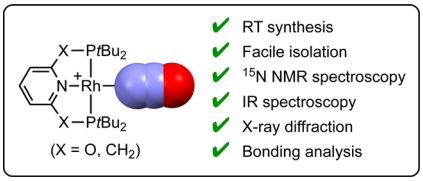


**Characterisation? NNO worries**: The synthesis and comprehensive characterisation of two rhodium(I) complexes of nitrous oxide are reported. These normally elusive adducts are stable in the solid state and persist in solution at ambient temperature.

  